Validation of new microvolume Couette flow linear dichroism cells

Rachel Marrington,[a] Timothy R. Dafforn,[b] David J. Halsall,[c] James I. MacDonald,[d] Matthew Hicks[a] and Alison Rodger*[a]

Received 5th May 2005, Accepted 28th September 2005
First published as an Advance Article on the web 14th October 2005
DOI: 10.1039/b506149k

Long molecules such as fibrous proteins are particularly difficult to characterise structurally. We have recently designed a microvolume Couette flow linear dichroism (*LD*) cell whose sample volume is only 20–40 μL in contrast to previous cells where the volume of sample required has typically been of the order of 1000–2000 μL. This brings the sample requirements of *LD* to a level where it can be used for biological samples. Since *LD* is the difference in absorption of light polarised parallel to an orientation direction and perpendicular to that direction, it is the ideal technique for determining relative orientations of subunits of *e.g.* fibrous proteins, DNA–drug systems, *etc.* For solution phase samples, Couette flow orientation, whereby the sample is sandwiched between two cylinders, one of which rotates, has proved to be the optimal technique for *LD* experiments in many laboratories. Our capillary microvolume *LD* cell has been designed using extruded quartz rods and capillaries and focusing and collecting lenses. We have developed applications with PCR products, fibrous proteins, liposome-bound membrane proteins, as well as DNA–dye systems. Despite this range of applications, to date there is nothing reported in the literature to enable one to validate the performance of Couette flow *LD* cells. In this paper we establish validation criteria and show that the data from the microvolume cells are reproducible, vary by less than 1% with sample reloading, follow the Beer–Lambert law, and have signals linear in voltage over a wide voltage range. The microvolume cell data are consistent with those from the large-volume cells for DNA samples. Surprisingly, upon extending the wavelength range by adding the intercalator ethidium bromide, the spectra in the microvolume and large-volume cells differ by a wavelength dependent orientation parameter. This wavelength variation was concluded to be the result of Taylor-vortices in the large-volume cells which have inner rotating cylinders in our laboratory. Thus the microvolume *LD* cells can be concluded to provide better data than our large-volume *LD* cells, though the latter are still to be preferred for titration series as it is extremely difficult to add sample to the capillary cells without introducing artefacts.

Introduction

Linear dichroism (*LD*) is a differential polarised absorption spectroscopy technique in which molecules in a sample are oriented and then the difference in absorption of light polarised in orthogonal directions (one of which is the orientation direction) is determined. Thus it is the ideal technique for studying classes of long biomacromolecules for which it is intrinsically difficult to gain structural information using more commonly available structural characterisation techniques such as NMR and X-ray diffraction. Recently we have reduced the sample requirements for *LD* by 2 orders of magnitude which has opened up a range of new applications for important biomacromolecules including PCR products,[1] fibrous proteins[2,3] (following early work in the 1970's (*e.g.* ref. 4, 5) but extending the wavelength and therefore the information gained), liposome-bound membrane proteins[6] as well as the more commonly studied DNA-dye systems *e.g.* ref. 7–11. Different methods of *LD* sample presentation exist for different types of sample, for example stretched film for small molecules, flow orientation, squeezed gel and electric field orientation for larger molecules.[6,9,12,13] However, for solution phase samples Couette flow orientation is most commonly used for the study of long biological macromolecules.

Couette flow *LD*, despite being used for structural studies for over 30 years, has not seen wide application, mainly because the required sample volume until recently made it very expensive to undertake experiments with biomacromolecules other than readily available DNAs. In addition few laboratories have been able to build their own cells. However, with our recent advances in Couette cell design both these issues have been solved.[14] Thus it is appropriate to consider the issue of *LD* cell validation to establish protocols before wide spread use in the biochemistry community is established. That is the aim of this paper.

Couette cells (Fig. 1) derive from the work of Maurice Frédéric Alfred Couette and Henry Reginald Arnulph Mallock, who in the late 1800's independently developed a

[a]*Department of Chemistry, University of Warwick, Coventry, UK CV4 7AL. E-mail: a.rodger@warwick.ac.uk; Fax: +44-24-76575795; Tel: +44-12-76574696*
[b]*Biosciences, University of Birmingham, Edgbaston, Birmingham, UK B15 2TT*
[c]*Department of Clinical Biochemistry, Box 232, Laboratory block Level 4, Addenbrooke's Hospital, Hills Road, Cambridge, UK CB2 2QQ*
[d]*Department of Mathematics, University of Warwick, Coventry, UK CV4 7AL*

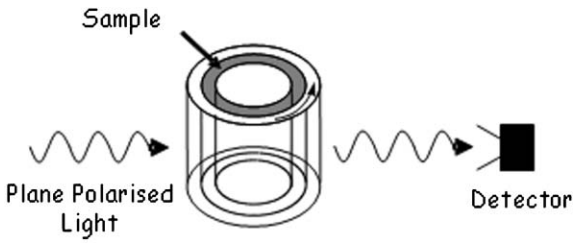

Fig. 1 Schematic diagram of *LD* Couette cell.

means to measure viscosity based on shearing a liquid between coaxial cylinders.[15–18] Since then there have been many applications of the Couette principle within the engineering and physics communities, the most notable example being that of Taylor.[19–21] Couette flow was developed further by Wada and Kozawa in 1964 into an apparatus for UV dichroism measurements.[22] In the 1960's–70's, flow *LD* was recognised as a useful technique and was used in the characterisation of fibrous proteins such as actin as well as probing the orientation of DNA and bound ligands.[23–28] The limitations of instrument design and technology with respect to the required sample volume (1–2 mL) and spectrometer design made it difficult to develop the technique further. Therefore Couette flow *LD* has been mainly restricted in application to DNA and DNA–drug systems as noted above.

The annular gap in Couette *LD* cells has typically been ~500 μm, though experiments using a 50 μm annular gap have been reported[2,5,6] which reduced the sample volume to 200 μL. The sample volumes required are still too large for applications such as analysis of PCR reactions, analysis of expensive biological samples including membrane proteins in liposomes, fibrous peptides, and proteins. This was the motivation for the new cell design which has also been used to develop the new technique of fluorescence detected flow *LD*[13] and to study the bacterial fibrous protein FtsZ.[29] In this paper we report experiments undertaken to show that the data from the new design of *LD* cell which requires only 25 μL sample are consistent with or better than those achieved with more traditional *LD* cells. The limitations of the new cells are also established.

Materials and methods

Design and construction of microvolume Couette *LD* cell

Two microvolume Couette *LD* cells have been designed and developed based on the same design, one being room temperature use only and the other having a heated metal jacket surrounding the capillary housing to enable steady-state thermostatting. The key features of the design are the use of an extruded quartz capillary (~5 mm outer diameter (o.d.) and ~3 mm inner diameter (i.d.)) as the outer rotating cylinder (Fig. 1), and a centrally mounted extruded quartz rod (o.d. dependent on annular gap and hence path length required, typically ~2.5 mm) as the inner stationary cylinder. The capillaries and rods were supplied by Enterprise-Q, Manchester, UK. The microvolume Couette *LD* cell was designed and built in collaboration with Crystal Precision Optics, Rugby, UK. The cell unit has been mounted on a base plate that has been designed specifically for Jasco *CD* spectropolarimeters with large sample compartments, though modifications to small compartments and other instrument bases are straightforward.

The main body of the microvolume Couette *LD* cell has been manufactured from laboratory and food industry specification stainless steel (Fig. 2). The bearings and drive spindle are also made from stainless steel and are designed to be dust and water resistant. The capillary units are demountable for removal during cleaning and sample loading. In this work the capillaries are sealed at the base with Araldite Rapid® and held in position in the metal base unit by an 'O'-ring. A motor is used to drive the 'O'-ring and in turn the capillary. This is controlled electronically by an EP-603 (0–30 V) power supply, adapted to allow more precise measurements (two decimal places) of applied voltage by the addition of a 10-turn potentiometer. A quartz rod is held within a Teflon® unit that is inserted into the metal lid. Before operation, the complete lid unit is inserted into the capillary and screwed securely into place (Fig. 2). This design enables different diameter rods to be used within the microvolume Couette cell.

Fig. 3(a) shows a photograph of the microvolume Couette flow *LD* cell and Fig. 3(b) shows a schematic diagram of the

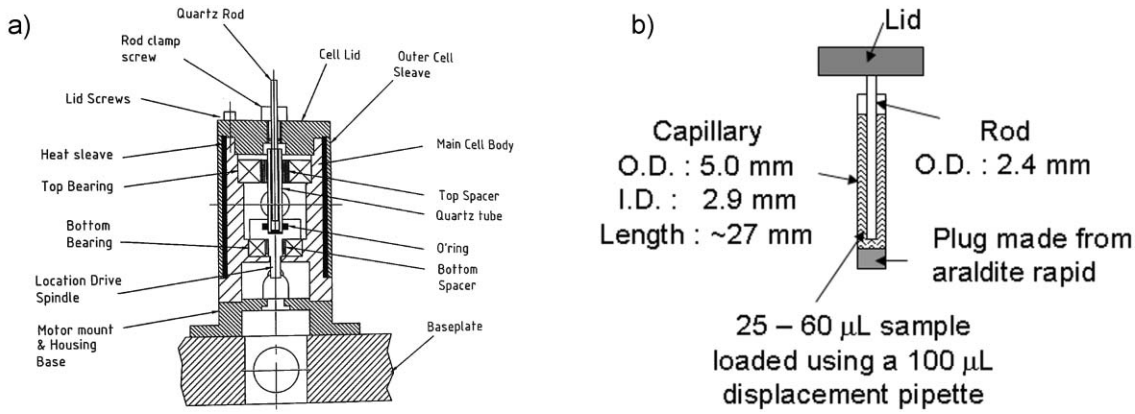

Fig. 2 (a) General arrangement drawing showing detail of quartz microvolume Couette flow *LD* cell and (b) schematic diagram showing the capillary and rod assembly in the microvolume Couette *LD* cell.

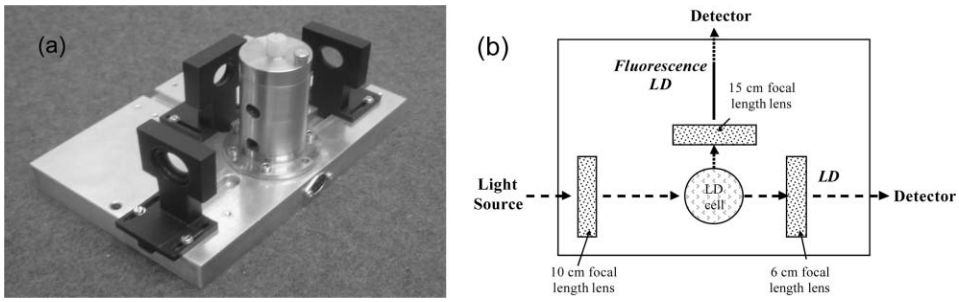

Fig. 3 (a) Photograph of microvolume Couette flow *LD* cell and (b) schematic diagram of microvolume Couette flow *LD* cell. Normal use has the detector on the right hand side; fluorescence-detected *LD* has the photomultiplier tube relocated to the top position.

unthermostatted cell (including the option for fluorescence detection[14]). A 2.54 cm diameter × 10 cm focal length uncoated lens (supplier Edmund Optics®) is placed 10 cm in front of the centre of the rod to ensure that the light is only incident on the middle of the capillary; and a second post-sample focusing lens (2.54 cm diameter × 6 cm focal length) is placed after the sample to focus the diverging light beam onto the photomultiplier tube (this has the added advantage of reducing the loss of light due to scattering by the large molecules often present in the samples for *LD* experiments). The base unit of the microvolume Couette *LD* cell has three slideways to hold the lens holders and to enable them to be finely adjusted by linear movements.

Thermostatted microvolume Couette LD cell

The thermostatted microvolume Couette *LD* cell is a development of the microvolume Couette *LD* cell, with the main difference being the addition of a thermostatted metal jacket with silicon rubber and fibreglass heater pads wrapped around the capillary unit, a temperature probe and a controller. The temperature controller was calibrated to allow the temperature to be set within the operating range (room temperature to ~60 °C). Once a temperature has been programmed, the controller will allow input current to the heater pad to raise the temperature up to near this temperature. The temperature probe is located on the top surface of the capillary unit, and measures the temperature of the steel housing (note, this is not the centre of the cell). When the preset temperature is close to being achieved, the controller switches from a continuous current input to an intermittent current input which holds the set temperature to ±0.2% of the set temperature. Higher temperatures require a longer equilibration time. For example in order to heat the capillary to 63 °C, the cell and temperature unit had to be left for an hour and a half (Fig. 4). The motor should be turned on during the equilibration period as the heat generated from the motor causes a net temperature increase in the sample of ~3 °C, and this should be taken into account when setting the temperature. For example if a temperature of 37 °C is required the temperature controller should be set to 34 °C.

Large-volume Couette LD cell

The large-volume 500 μm annular gap cells used for comparison purposes included the original one (LV Cell 1) from our laboratory, whose design is reported in ref. 12 and a more recently designed version of this (LV Cell 2) where the outer stationary cylinder is a quartz capillary held in place within a stainless steel housing, with gaps for the light to pass through the sample, and a central rotating quartz cylinder.

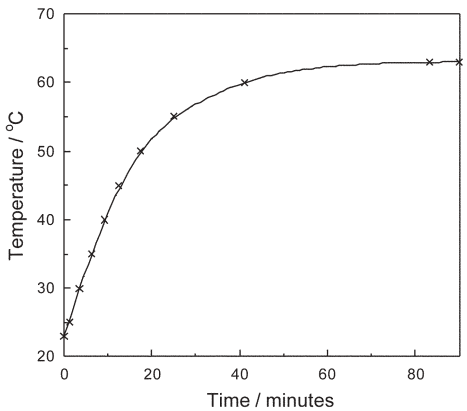

Fig. 4 The temperature of the thermocouple as a function of time from switching on the heater in the thermostatted microvolume Couette *LD* cell.

Experiments for validation of performance of Couette flow LD cells

Calf thymus-DNA (ct-DNA highly lyophilised from Sigma) was dissolved in high purity water (18.2 mΩ) and used for most experiments summarised below. For investigating the larger wavelength range, 750–200 nm, DNA–ethidium bromide solutions were used at concentrations specified below. For LV Cell 1 2000 μL and for LV Cell 2 1000 μL of sample were used at a voltage of 2 V (unless otherwise stated). For the microvolume Couette *LD* cell, samples were individually prepared with volumes of 40 μL placed into the capillary and a voltage of 4 V was used in all experiments, unless otherwise stated. A Gilson air displacement pipette (P100) was used for the loading of capillaries. Volumes of 25–60 μL can be used in conjunction with a ~2.5 mm outer diameter rod. A Jasco J-715 with large sample compartment that has been adapted for *LD* measurements was used for all *LD* experiments. Instrumental parameters for experiments with ct-DNA alone and ct-DNA–ethidium bromide, in both full wavelength (spectrum measurement) and kinetics (time course measurement) are given in Table 1.

Table 1 Parameters used on the Jasco J-715 spectropolarimeter for both wavelength scanning measurements and time course measurement. Parameters in parentheses were those used for calculation of revolutions per minute (rpm) for the microvolume Couette *LD* cell

	DNA alone	DNA–ethidium bromide
Spectrum measurement		
Wavelength/nm	350–190	600–190
Scanning speed/nm min^{-1}	200	500
Response/s	0.5	0.25
Data pitch/nm	0.5	0.5
Band width/nm	2.0	2.0
No. of accumulations	4	4
Time course measurement		
Time/s	0–900 (0–60)	
Response/s	0.5 (0.5 ms)	
Data pitch/s	1 (10 ms)	
Band width/nm	2.0	
Wavelength monitored/nm	259	
No. of accumulations	1	

Error analysis for both the large-volume Couette *LD* cell and microvolume Couette *LD* cell were carried out using both the time course measurement and spectrum measurement programs within the Jasco software. The error in a single analysis was determined by calculating the relative standard deviation (RSD) across all data points within a time envelope of 15 minutes. Multiple analyses were simulated in the LV Couette *LD* cells by stopping and starting the power supply, and in the microvolume Couette *LD* cell by stopping the power supply, emptying the capillary, and then refilling it with the same DNA solution. This experiment was repeated 15 times using full-wavelength analysis and the RSD of the signal maximum at 259 nm (LD_{259}) was calculated. The effect of bandwidth was ascertained by visual inspection of full-wavelength spectra of ct-DNA with different bandwidths and all other parameters as in Table 1. Rotation speeds were calculated for the microvolume Couette *LD* cell by filling the capillary with ct-DNA (200 μM) and then marking the outside of the capillary with a marker pen. The frequency with which the light was interrupted during a time course measurement program (using the parameters in parentheses in Table 1) was then determined. (The mark passes through the light beam twice per revolution.) The supplied voltage was increased in 0.5 V increments from 0 V to 6 V. Different concentrations of ct-DNA were prepared for evaluation of the Beer–Lambert law, ranging from 0–1000 μM.

Concentrations of ct-DNA were determined spectrophotometrically using the molar absorption coefficient per base of $\varepsilon_{259} = 6600\ M^{-1}\ cm^{-1}$.[30] This in turn, along with absorbance data measured independently and scaled for path length differences, was used to determine the sample orientation parameter (S), by rearrangement of eqn (1) where LD^r is the reduced linear dichroism and A the absorbance. The angle between the macroscopic orientation axis and the transition moment termed α was assumed to be 86°.[7]

$$LD^r = \frac{LD}{A} = \frac{3}{2}S\left(3\cos^2\alpha - 1\right) \quad (1)$$

Absorbance spectra in a 1 cm path length quartz cuvette were also collected for all solutions to enable LD^r values to be calculated. A Jasco V-550 UV spectrometer was used for absorbance measurements using the same wavelength and data pitch as that for *LD*.

Results and discussion

Baselines

The capillaries were found to be optically uniform by measuring baseline spectra with different capillary orientations. Thus it is possible to collect a baseline spectrum either by simply stopping the rotating capillary (and hence the alignment force) or using a water–buffer solution with the cell rotating. This situation is in contrast to LV Cell 1 and LV Cell 2 where the baseline measurement has to average over the rotating cell due to variation in the quartz cores as they rotate. It should be noted that it is important to place the rod in the capillary in the same orientation on each occasion as the rod is not as optically uniform as the capillary. If one is working with a capillary cell with light scattering samples, measuring the baseline on the non-rotating sample usually produces better spectra.

Sample volume

Fig. 5 shows that the same *LD* signal has been achieved in the capillary cell with all sample volumes from 25–60 μL. However, it should be noted that the useable volume range is entirely dependent on the amount of Araldite Rapid® used and the location of the rod. The required minimum volume can be calculated for a given capillary from the height of the light beam, the internal volume of the capillary to that height, and the volume of the rod to that height (using capillary internal diameters and rod outer diameters as measured using a micrometer). However, a simple experiment of a number of independently loaded samples should be used to check this and the reproducibility of the loading procedure. Volumes of ~40 μL are used for most experiments reported herein as the smaller volumes are more prone to being loaded with bubbles. Because the capillaries are removable, it is possible to recover the sample.

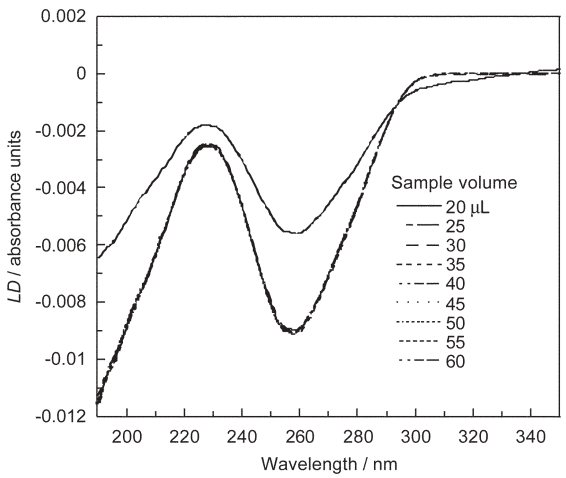

Fig. 5 *LD* spectra of different volumes of ct-DNA (~200 μM) in a capillary.

Sample loading

A series of experiments with ct-DNA showed that not only is a flow gradient established upon rotation of the capillary, but a concentration/size gradient of matter is created. We observed that when the rod is removed, the sample it lifts out is more concentrated than what is left behind. Therefore, all samples should be individually prepared with great care for analysis or reloading. For a series of experiments it is advisable to use the same capillary and rod.

Voltage and rpm relationship

The relationship between voltage and rpm was established by counting the number of revolutions of the capillary by monitoring the period in the HT voltage trace (which indicates absorbance) of a marked capillary, taking into account that the marker will pass through the light beam twice in one revolution (Fig. 6). A linear relationship was observed between rpm and voltage at voltages above 3 V (which fortuitously corresponds to 3000 rpm). It was also found that the signal to noise ratio improves with increasing voltage, with the optimum being 4 V or greater if the sample allows (*i.e.* no bubble formation or turbulence, see below). The minimum voltage of 3 V for a linear relationship between rpm and voltage will depend on individual motors, units and systems under investigation. 4 V is used in this work unless otherwise stated.

Bandwidth dependence of spectra

Bandwidths of 0.1; 0.2; 0.5; 1.0; 2.0; 5.0 and 10.0 nm with the Jasco J-715 were investigated using ct-DNA and the capillary *LD* cell. All bandwidths gave the same spectral shape but it was observed that only 1.0; 2.0 and 5.0 nm bandwidths gave spectra of the same intensity (within tolerances of 1%). There was a large decrease in spectral intensity when using a 10 nm bandwidth (presumably because the size of the light beam is wider than the rod in the far UV region), and the signal to noise ratio was worse when using smaller bandwidths (0.1–0.5 nm). A bandwidth of 2 nm is recommended for use with the microvolume Couette *LD* cell and Jasco spectropolarimeters.

Dependence of capillary LD signal on sample concentration

The validity of the Beer–Lambert law was investigated by measuring LD_{259} of different concentrations of ct-DNA (Fig. 7) in the capillary *LD* cell. It can be seen that all the data points lie on a straight line which indicates that the Beer–Lambert law is obeyed for *LD* of ct-DNA with concentrations up to 1000 μM at 4 V.

Full wavelength range data

Ethidium bromide bound to ct-DNA was used to show that *LD* spectra could be collected in the visible region of the spectrum. A titration series (samples individually prepared) of ethidium bromide complexed to ct-DNA is shown in Fig. 8. The spectra are in accord with literature data,[31] but, slight differences were observed compared with the control experiments with the large-volume Couette *LD* cell (see below).

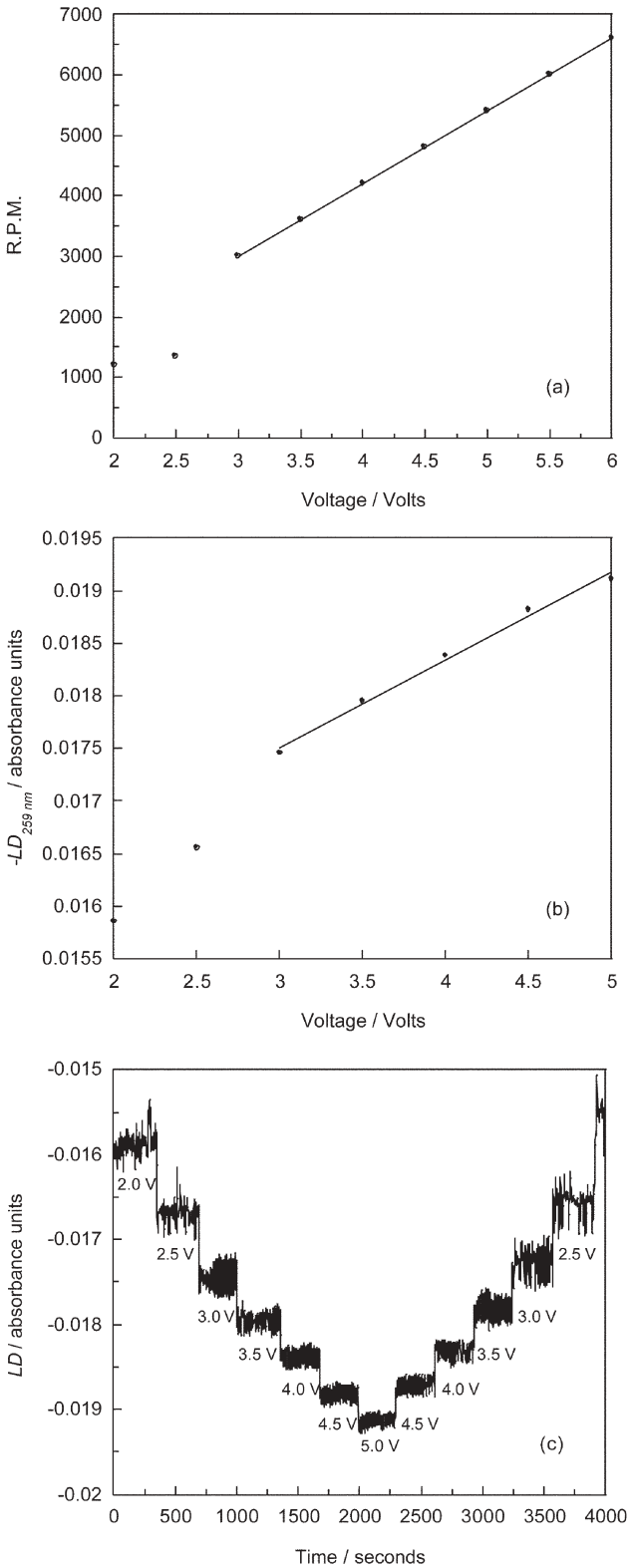

Fig. 6 (a) The relationship between voltage and rpm of the microvolume Couette *LD* cell, (b) the relationship between LD_{259} and voltage and (c) *LD* intensity variation at different voltages. All experiments were carried out using ct-DNA (~200 μM).

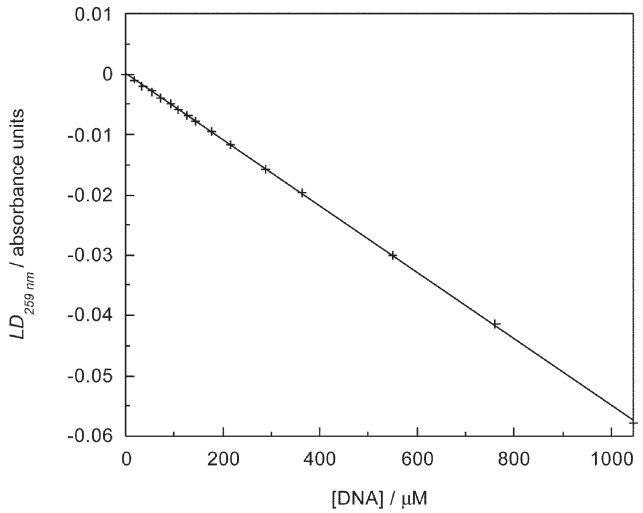

Fig. 7 LD_{259} *versus* DNA concentration in the microvolume Couette *LD* cell at 4 V.

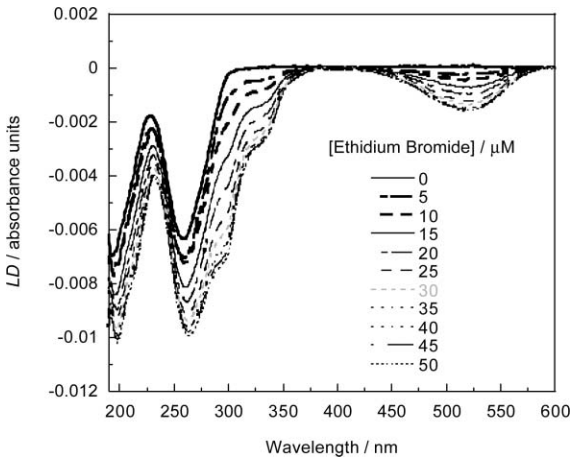

Fig. 8 *LD* spectra of ct-DNA (200 μM) and different concentrations of ethidium bromide (0–50 μM) in sodium cacodylate buffer (10 mM) pH 7.0 and NaCl (10 mM).

Capillary cell *versus* large-volume cell for DNA

The microvolume Couette cell was evaluated against LV Cells 1 and 2 to investigate cell to cell reproducibility. LD_{259} as a function of DNA concentration was determined for the capillary cell and LV Cell 2 (Fig. 9). The microvolume Couette *LD* cell follows the Beer–Lambert law somewhat better than LV Cell 2 (but its signal is smaller as it has a smaller path length and also smaller orientation effect than LV Cell 2 (though not LV Cell 1)). LV Cell 1, which is the older of the two LV cells, deviates from the capillary cell at low wavelength.

DNA and ethidium bromide cell to cell comparison

Fig. 10 shows that it is not possible to simply rescale the microvolume Couette cell data to directly overlay with the LV Cell 2 for DNA–ethidium bromide (*i.e.* over a wide wavelength range). This was found also to be the case for different ratios of DNA : ethidium bromide. In order to determine whether this was an effect of the different shear forces being applied to the samples, the shear force on both cells was calculated following the model for shear force within small annular gaps given by Nordén *et al.*[10]

$$G \approx \frac{\omega r_o}{r_o - r_i} \quad (2)$$

where G is the shear force, ω the angular velocity and r_o and r_i the radii of the outer and inner cylinders respectively. The velocity profile is shown in Fig. 11.

The microvolume Couette cell, assuming 3 V (minimum voltage required for linearity of DNA signal) is equivalent to 3000 rpm, *i.e.* 310 rad s^{-1}, and r_o and r_i are 1.45 and 1.2 mm respectively, resulting in a shear force of $\sim$1800 s^{-1}. An approximately equivalent shear force in LV Cell 2 requires ω = 70.1 rad s^{-1} using values of r_o and r_i of 13 and 12.5 mm; this equates to an rpm value of 670 rpm and a voltage of 1.62 V. LD^r data were therefore collected for both systems

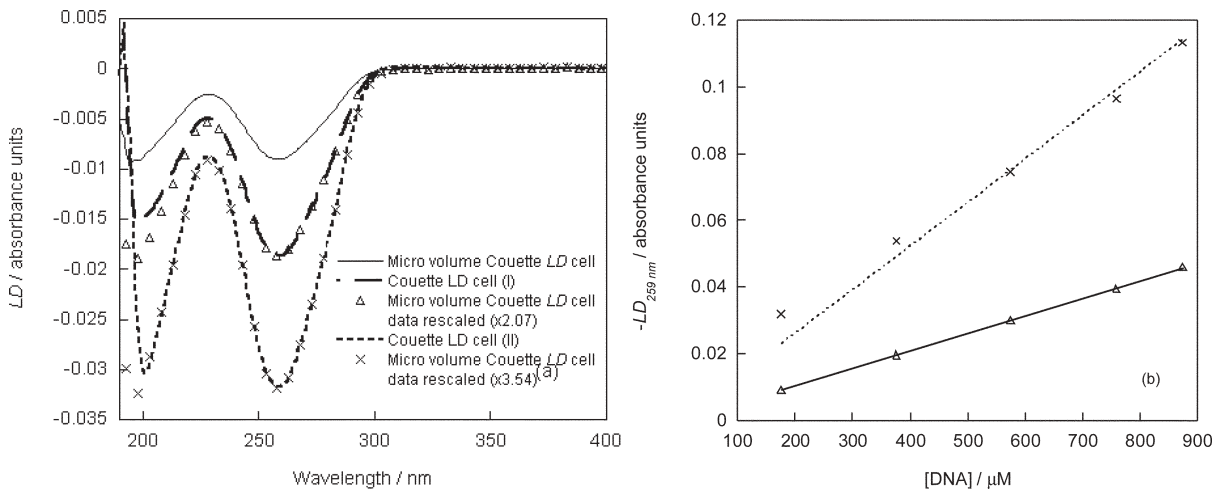

Fig. 9 *LD* of DNA (176 μM). (a) Wavelength scans in microvolume Couette *LD* cell (—), LV Cell 1 (– – – –) and LV Cell 2 (- - -), with rescaling of the microvolume Couette *LD* cell spectrum to overlay at 259 nm on LV Cell 1 (△ △ △) and LV Cell 2 (× × ×) spectra; (b) 259 nm magnitudes for microvolume Couette LD cell (solid line) and LV Cell 2 (dotted line).

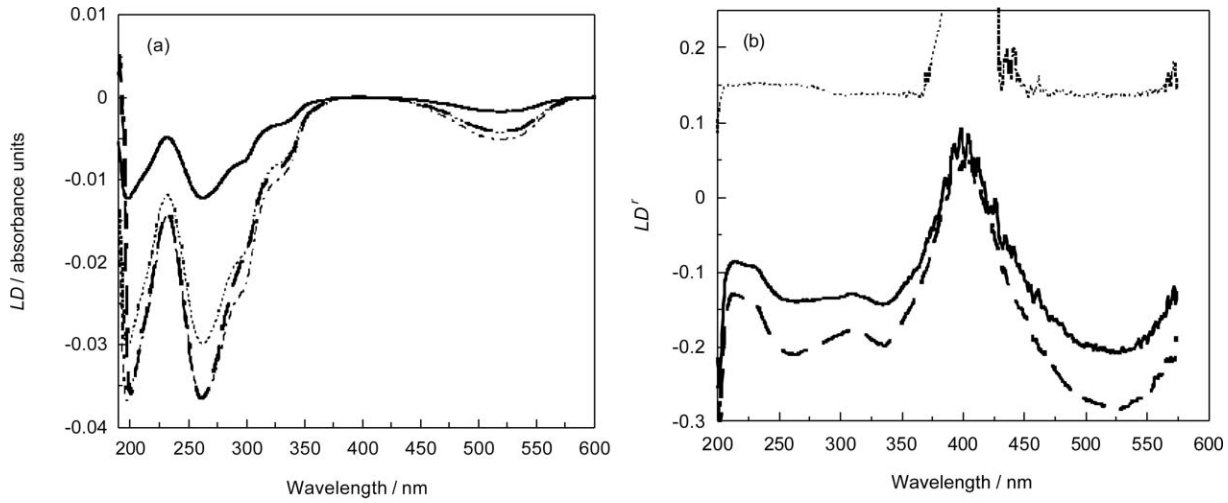

Fig. 10 (a) *LD* spectra of DNA (176 μM) and ethidium bromide (50 μM) in NaCl (10 mM) and sodium cacodylate buffer (10 mM) pH 7.0 in the microvolume Couette cell (—) and LV Cell 2 (– – –). The *LD* spectrum for the microvolume Couette *LD* cell has been rescaled to match the signal of LV Cell 2 at 259 nm (- — -) and at 520 nm (·····). (b) LD^r spectra of *LD* spectra in part (a) and the ratio of Cell 2 to capillary cell *LD* (divided by 10) (·····).

using similar shear forces (Fig. 10). The spectra still show the same differences, so the discrepancy is not a function of shear force. The LD^r spectra and the ratio between the LD^r's of the two cells are constant in the DNA region and constant across the ethidium region—but with, relatively, the microvolume cell having the smaller signal for DNA or the larger for ethidium. At lower ethidium loadings the same effect is observed, but in addition the long-wavelength ethidium band has a slightly lower ratio than the shorter wavelength bands. Another key difference between the two cells is the fact that LV has an inner rotating cylinder while the microvolume cell has an outer rotating one. The former has a more complicated flow behaviour as summarised in Fig. 12 and discussed below.

The most definitive work on Couette systems after the time of Mallock[17] and Couette[15] was that of Taylor who investigated the stability of a viscous flow with two cylinders rotating in the same direction and in opposite directions and later went on to conclude that if the outer cylinder only rotates, the flow is more stable than if only the inner cylinder rotates.[16,19,21] Taylor distinguished two broad categories of fluid states by their symmetry under rotation and reflection: laminar flow and turbulent flow. Laminar flow (also known as Couette flow) is the most stable flow and usually occurs at low flow velocities. It is this state that is required for *LD*. In turbulent flow, vortices, eddies and wakes make the flow unpredictable. Between laminar and turbulent flow a state called Taylor-vortex flow exists made up of helical vortices. A useful dimensionless variable to summarise the relative significance of the viscous effect compared to the inertia effect is given by the Reynolds number (R_e) (named after Osbourne Reynolds[32,33]). R_e, in the form applicable for a fluid in the annulus between two concentric cylinders, is defined

$$R_e = \frac{\omega_1 r_1 \delta}{\nu} \tag{3}$$

where ω_1 is the angular velocity of one rotating cylinder in rad s^{-1}, r_1 is the radius of that rotating cylinder in m, δ is the gap width $|r_2 - r_1|$ in m, and ν the kinematic viscosity in $m^2\ s^{-1}$ (kinematic viscosity is equal to absolute or dynamic viscosity divided by density).[34] A complex transition diagram has been published by Andereck *et al.*[36] in 1986 (Fig. 12) to summarise when each state is expected.

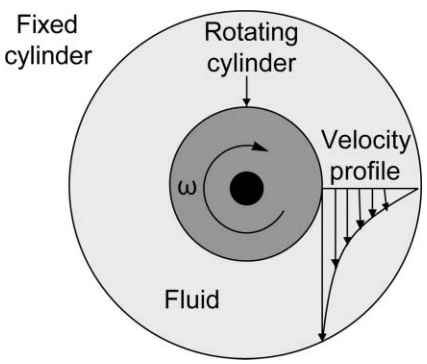

Fig. 11 Plan of a Couette cell showing the velocity profile of a fluid contained between concentric cylinders as the inner cylinder rotates, redrawn from Wilkes.[35] The arrows represent the direction of the flow at the point where the axes touch the inner cylinder and the lengths represent the velocity.

The significance of this diagram for the microvolume and LV Cells is summarised in Table 2 if we assume: (1) the solution is or resembles water, so has a kinematic viscosity[34] of $10^{-6}\ m^2\ s^{-1}$ and (2) DNA may be represented as an infinite length cylinder. In particular, at least in principle, the outer rotating cell should remain in the Couette flow domain whereas the inner rotating cell is close to the regime of Taylor-vortex flow. In such a flow state the fluid forms cylindrical vortices about the flow direction. This would mean that the DNA is oriented in toroids about the flow direction, with the regions of ethidium intercalation orienting more effectively. Somewhat perversely, the DNA molecules so oriented will reduce the orientation parameter for ethidium relative to the DNA bases (in Couette flow it is the other way

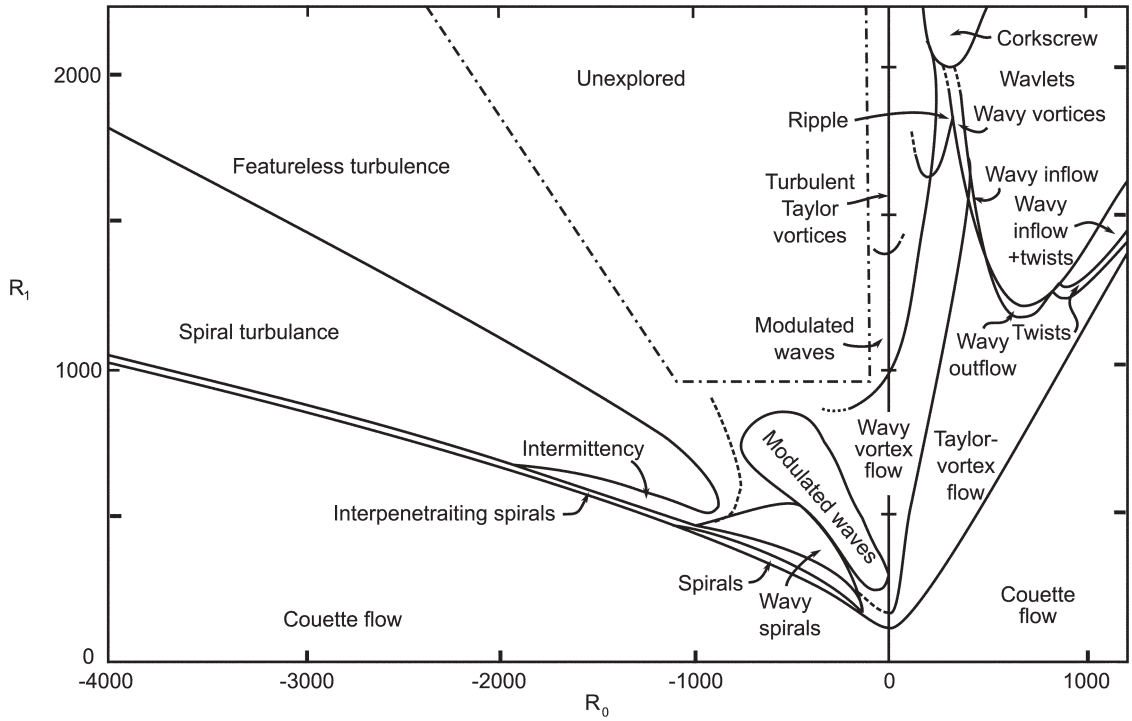

Fig. 12 Diagram of Taylor–Couette flow states from that of Andereck *et al.*,[36] where R_i and R_o are the inner and outer cylinder Reynolds numbers respectively.

Table 2 Comparison of fluid flow in the LV Cell 2 and the microvolume Couette *LD* cell for solutions of the same kinematic viscosity as that of water

		ω				
	High/low speed of rotation	/rpm	/rad s^{-1}	R_o	R_i	Flow state
Couette *LD* cell	Low (1 V)	300	31.4	0	196.25	Couette flow–Taylor-vortex flow
$r_1 = 0.0125$ m	High (4 V)	2000	209.4	0	1308.75	Turbulent flow
$\delta = 0.0005$ m						
Microvolume Couette *LD* cell	Low (3 V)	3000	314.2	113.90	0	Couette flow
$r_1 = 0.00145$ m	High (6 V)	6600	691.2	250.5	0	Couette flow
$\delta = 0.00025$ m						

round since the DNA is stiffer), resulting in relative reduction of the orientation parameter for ethidium-bound DNA *versus* free DNA.

Conclusions

The aim of the work reported in this paper has been to establish validation protocols for *LD* and in particular to determine to what extent the data collected in the newly designed microvolume capillary *LD* cells can be trusted. The most important result is that the new configuration with lenses to focus the light beam on the capillary does not cause any artefacts in the observed spectrum compared with older cells where this is not required. The data from the microvolume cell follow the Beer–Lambert law and have signals linear in voltage after a threshold value. The data are reproducible, with only $\sim$1% variation with careful reloading of samples, and can be used over a wide bandwidth range. The data from previously designed large-volume cells are consistent with those from the capillary for pure DNA samples. However, for DNA with ethidium bromide intercalated in some DNA binding sites the spectra show different orientation parameters in the DNA base and bound ethidium regions. This proved not to be due to differences in flow velocities, but rather to be intrinsic features of the designs of the cells. The microvolume cells have an outer rotating capillary and inner stationary rod, so their fluid flow is more stable and the data more reliable from the microvolume cells than those from inner rotating large-volume cells that have been previously used in our laboratory. At least in principle, the capillary cells maintain Couette flow which means we are indeed orienting the samples along the direction of flow, in contrast to the LV cells where it seems that some element of Taylor-vortex flow is operating even at low voltages. However, it should be noted that in practice bubbles readily form in the capillary cells at high voltages in samples containing detergents. Additional advantages of the microvolume cells are that it has been possible to design a thermostatted jacket for the cell for steady state temperature work, it requires only $\sim$25 μL sample (with the size of Araldite plug we choose to use), though $\sim$40 μL makes sample loading

easier. It should be noted, however, that the large-volume cells have an undeniable advantage when titration experiments need to be undertaken.

Acknowledgements

The collaboration of Crystal Precision Optics, Rugby UK has been a key factor in the design and building of the micro-volume capillary cells and is gratefully acknowledged. Syngenta UK (PhD studentship to RM), the BBSRC (REI20503), The Association of Clinical Biochemists, and the EPSRC (GR/T09224/01) are also thanked for financial support for this work. Jim MacDonald is acknowledged for drawing Fig. 12. The referees' careful work has also been very valuable.

References

1 T. R. Dafforn, D. J. Halsall and A. Rodger, *Chem. Commun.*, 2001, 2410–2411.
2 T. R. Dafforn, J. Rajendra, D. J. Halsall, L. C. Serpell and A. Rodger, *Biophys. J.*, 2004, **86**, 404–410.
3 T. R. Dafforn and A. Rodger, *Curr. Opin. Struct. Biol.*, 2004, **14**, 541–546.
4 T. Yanagida, M. Taniguchi and F. Oosawa, *J. Mol. Biol.*, 1974, **90**, 509–522.
5 M. Taniguchi and R. Kuriyama, *Biochim. Biophys. Acta*, 1978, **533**, 538–541.
6 A. Rodger, J. Rajendra, R. Marrington, M. Ardhammar, B. Nordén, J. D. Hirst, A. T. B. Gilbert, T. R. Dafforn, D. J. Halsall, C. A. Woolhead, C. Robinson, T. J. Pinheiro, J. Kazlauskaite, M. Seymour, N. Perez and M. J. Hannon, *Phys. Chem. Chem. Phys.*, 2002, **4**, 4051–4057.
7 A. Rodger and B. Nordén, *Circular Dichroism and Linear Dichroism*, Oxford University Press, Oxford, UK, 1997.
8 M. J. Hannon, V. Moreno, M. J. Prieto, E. Molderheim, E. Sletten, I. Meistermann, C. J. Isaac, K. J. Sanders and A. Rodger, *Angew. Chem.*, 2001, **40**, 879–884.
9 B. Nordén, *Appl. Spectrosc. Rev.*, 1978, **14**, 157–248.
10 B. Nordén, M. Kubista and T. Kurucsev, *Q. Rev. Biophys.*, 1992, **25**, 51–170.
11 P. Chou and W. C. Johnson, *J. Am. Chem. Soc.*, 1993, **115**, 1205–1214.
12 A. Rodger, *Methods Enzymol.*, 1993, **226**, 232–258.
13 L. B. A. Johansson and A. Davidsson, Analysis and Application of Linear Dichroism on Membranes—Description of a Linear-Dichroism Spectrometer, *J. Chem. Soc., Faraday Trans. 1*, 1985, **81**, 1375–1388.
14 R. Marrington, T. R. Dafforn, D. J. Halsall and A. Rodger, *Biophys. J.*, 2004, **87**, 2002–2012.
15 M. Couette, Etudes sur le frottement des liquides, *Ann. Chim. Phys.*, 1890, **6**, 433–510.
16 R. J. Donnelly, *Phys. Today*, 1991, 32–39.
17 A. Mallock, *Proc. R. Soc. London*, 1888, **45**, 126–132.
18 A. Mallock, *Philos. Trans. R. Soc. London, Ser. A*, 1896, **187**, 41–56.
19 G. I. Taylor, *Proc. R. Soc. London, Ser. A*, 1923, **223**, 289–343.
20 G. I. Taylor, *Proc. R. Soc. London, Ser. A*, 1936, **157**, 546–564.
21 G. I. Taylor, *Proc. R. Soc. London, Ser. A*, 1936, **157**, 565–578.
22 A. Wada and S. Kozawa, *J. Polym. Sci., Part A*, 1964, **2**, 853–864.
23 S. Higashi, M. Kasai, F. Oosawa and A. Wada, *J. Mol. Biol.*, 1963, **7**, 421–430.
24 J. Hofricheter and W. Eaton, *Annu.Rev. Biophys. Bioeng.*, 1976, **5**, 511–560.
25 F. Oosawa, Y. Maeda, S. Fujime, S. Ishiwata, T. Yanagida and M. Taniguchi, *J. Mechanochem. Cell Motil.*, 1977, **4**, 63–78.
26 A. Wada, *Appl. Spectrosc. Rev.*, 1972, **6**, 1–30.
27 A. Wada, *Biopolymers*, 1964, **2**, 361–380.
28 M. Taniguchi, A. Yamaguchi and T. Taniguchi, *Biochim. Biophys. Acta*, 1971, **251**, 164–171.
29 R. Marrington, E. Small, A. Rodger, T. R. Dafforn and S. Addinall, *J. Biol. Chem.*, 2004, **47**, 48821–4882.
30 R. D. Wells, J. E. Larson, R. C. Grant, B. E. Shortle and C. R. Cantor, *J. Mol. Biol.*, 1970, **54**, 465–497.
31 B. Nordén and F. Tjerneld, *Biophys. Chem.*, 1976, **4**, 191–198.
32 O. Reynolds, *Proc. R. Soc. London*, 1883, **35**, 84–99.
33 O. Reynolds, *Philos. Trans. R. Soc. London*, 1883, **174**, 935–982.
34 M. C. Potter and D. C. Wiggert, *Mechanics of Fluids*, Brooks/Cole Thomson Learning, Pacific Grove, CA, 2002.
35 J. O. Wilkes, *Fluid Mechanics for Chemical Engineers*, Prentice Hall PTR, Upper Saddle River, NJ, 1999.
36 C. D. Andereck, S. S. Liu and H. L. Swinney, *J. Fluid Mech.*, 1986, **164**, 155–183.